

# Synthesis and characterization of SnO<sub>2</sub> nanowires

Author: Roger Pieres Termes

*Facultat de Física, Universitat de Barcelona, Diagonal 645, 08028 Barcelona, Spain.*

Advisor: Paolo Pellegrino, Guillem Domènech Gil

**Abstract:** In this study, tin dioxide (SnO<sub>2</sub>) nanowires (NWs) have been synthesized using a Chemical Vapor Deposition (CVD) furnace. The optimal growth conditions were 900 °C, with 1 g of Sn as the precursor and 100 Standard Cubic Centimeters per Minute (sccm) of 1000 parts per million (ppm) of oxygen (O<sub>2</sub>) diluted in argon (Ar) as the carrier gas. Their characterization has been done using Scanning Electron Microscopy (SEM) and gas sensing properties under controlled UV light intensity have been studied in a gas chamber. Regarding gas measurements, the sensor's behaviour was studied with and without the influence of UV light in different atmospheres using a 360 nm LED. In dry air, the I(V) characteristics of the sensor were analysed. It was observed that the sensor exhibited Schottky behaviour (metal-semiconductor-metal junction) when the LED intensity was below 3 mA, and ohmic behaviour for intensities equal or above 3 mA. Subsequently, the sensor's response was examined in the presence of wet air, at different fixed levels of relative humidity (RH), and the response and response time were studied under increasing UV illumination. It was found that both the response time and the relative change in electrical resistance decreased as the LED intensity or humidity increased. Finally, the sensor's behaviour in dry air with humidity pulses (varying RH) was investigated. It was observed that the sensor exhibited n-type behaviour when not illuminated and p-type behaviour when illuminated. In addition, the sensor was exposed to methane (CH<sub>4</sub>) pulses, showing no response.

## I. INTRODUCTION

In recent years, gas sensors have garnered significant interest due to their utility in industrial process control and environmental analysis. Currently, the market offers gas sensors based on metal oxide semiconductors, such as SnO<sub>2</sub>. Depending on the metal used, these gas sensors detect certain gases better than others. SnO<sub>2</sub> is particularly interesting because it can detect combustion gases like carbon monoxide (CO), hydrogen (H<sub>2</sub>) and CH<sub>4</sub>. To optimize these type of sensors, extensive research is being conducted. The sensors currently available on the market operate with a thin film, and, since the sensitivity depends on the contact surface with the gas, efforts are being made to increase their surface area. One way to increase the surface-to-volume ratio, is to fabricate a gas sensor based on nanowires (NWs). Therefore, this study will focus on the fabrication and characterization of SnO<sub>2</sub> NWs with the aim of developing a gas sensor, but, unlike previous studies reported in the scientific literature, this research intends to operate the sensor at room temperature using UV light instead of heating at 200 °C or above.

## II. THEORETICAL MODEL

### A. Gas Sensing

The physical principle that enables SnO<sub>2</sub> to detect gases is explained by the depletion zone model. SnO<sub>2</sub> is a semiconductor that exhibits n-type behaviour due to manufacturing imperfections. These imperfections result in oxygen vacancies, leading to unsatisfied bonds and unpaired

electrons (the ideal stoichiometric ratio should be Sn:O=1:2, but it is typically Sn:O=1:1.8). These unsatisfied bonds readily donate their electrons and act as donor levels near the conduction band (hence, the material behaves as an n-type semiconductor). Additionally, these unsatisfied bonds behave as active sites (only near the surface) for O<sub>2</sub> in the atmosphere to adsorb, forming oxygen ions (O<sub>2</sub><sup>-</sup>). These adsorbed ions capture the conduction band electrons, thereby modifying the material's conductivity. Moreover, capturing these electrons generates a positively charged region (depletion region) near the surface, creating an electric dipole and a surface potential barrier [1].

When a gas molecule reaches the SnO<sub>2</sub> surface, it reacts with the oxygen vacancies. Depending on the type of gas, we can differentiate between oxidizing gases and reducing gases. If the gas adsorbs on the substrate forming ions and capturing unpaired electrons, it is an oxidizing gas, such as O<sub>2</sub> or nitrogen dioxide (NO<sub>2</sub>). Conversely, if the gas reacts with the pre-adsorbed ions and removes them from the substrate, releasing electrons, it is a reducing gas, such as CO. Initially, at room temperature, the substrate surface is covered with O<sub>2</sub><sup>-</sup> in equilibrium with atmospheric O<sub>2</sub>, leaving a small fraction of oxygen vacancies available for another gas to adsorb. Under these conditions, the substrate is saturated, as most vacancies are filled, preventing the sensor from reacting with gases. Therefore, in many studies, the sensor is heated to provide sufficient thermal energy for the adhered oxygen molecules to desorb [2].

However, an interesting effect occurs if, instead of heating, the substrate is irradiated with UV light. When the substrate is illuminated with photons, their energy desorbs

---

\* Electronic address: rpierete7@alumnes.ub.edu

some of the adsorbed O<sub>2</sub> molecules, allowing other molecules to adsorb. This creates a steady-state dynamic of adsorption and desorption of both O<sub>2</sub> and the target gas molecules. If the target gas is an oxidizing gas, it will compete with O<sub>2</sub> for adsorption on the substrate. Conversely, if the target gas is a reducing gas, it will react with the adhered O<sub>2</sub><sup>-</sup> ions, causing them to desorb [2].

### B. Growing Process

Vapor-Liquid-Solid (VLS) mechanism involves evaporating a metallic precursor and transporting it using a gas to a substrate to grow one-dimensional structures, such as NWs. On this substrate, there is a metallic catalyst (Au in our case), previously deposited as a thin layer, that forms droplets when heated. The thickness of the deposited catalyst layer, and consequently the size of the catalyst droplets formed, is crucial because the diameter of the NWs will depend on it. Too thick layers will not promote droplets and, therefore, NWs will not grow.

When the metal reaches the substrate in the gas/vapor phase, it fuses with the gold droplets to form an eutectic alloy. As the metal continues to fuse with the gold droplets, they become saturated. Once supersaturation is reached, the metal begins to precipitate from beneath the droplet. The metal, both in the droplet and in the vapor phase, oxidizes and solidifies. The metal oxide beneath the droplet starts forming a one-dimensional structure, causing the droplet to move upward as it grows, due to the metal oxide being denser than the eutectic alloy and in a solid state. Fig.(1) illustrates the VLS growth process.

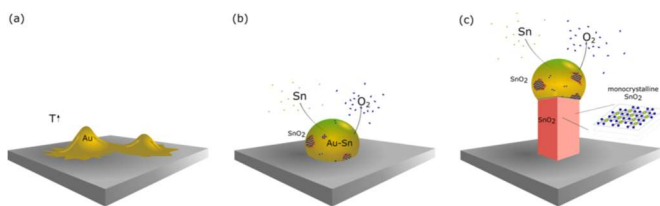


**FIG. 1:** (a) Gold droplets formed from the thin layer at high temperatures (between 600 °C and 1000 °C). (b) Fusion of gold droplets with Sn in presence of oxygen. (c) Precipitation and oxidation of Sn to form a monocrystalline SnO<sub>2</sub> NW [3].

## III. EXPERIMENTAL

### A. Chemical Vapour Deposition Growth

To manufacture the NWs, a Thermo Scientific Lindberg HTF55347C Blue M Tube Furnace (3 zones) was used. This furnace consists of a quartz tube surrounded by electrical resistances and insulated with refractory material, capable of reaching temperatures up to 1200 °C (though the maximum temperature for the tube used is approximately 1000 °C). Each zone can be assigned a specific temperature using the UP150 temperature controller and thermocouples positioned equidistantly along the furnace.

The quartz tube is connected on one end to two Mass Flow Controllers (MFCs) and on the other end to a vacuum pump in parallel with a unidirectional overpressure regulating valve. The vacuum pump operates through an adjustable manual valve that controls the vacuum rate. The MFCs are connected to two gas cylinders, one containing Ar and the other containing 1000 ppm of O<sub>2</sub> diluted in Ar.

The growth process is divided into four stages. In the first stage, a 10 mTorr vacuum is created inside the quartz tube. Ar is then injected at a flow rate of 100 sccm for 10 minutes.

In the second stage, the furnace begins to heat the tube. The heating is gradual, occurring over 20 minutes with a linear temperature increase. The target temperatures for the furnace are 800 °C, 900 °C, and 1000 °C.

In the third stage, the MFC switches to the gas cylinder containing 1000 ppm of O<sub>2</sub> diluted in Ar and injects it at 100 sccm for 2 hours. During this stage, the NWs start to grow.

Finally, in the fourth stage, the furnace begins to cool down following an exponential decay profile. For 1 hour, the MFC injects pure Ar at 100 sccm to stop the growth of the NWs.

The substrate used for NW growth is Si/SiO<sub>2</sub> (pieces of 5x5 mm<sup>2</sup>). For the fabrication of the gas sensor, a different substrate composed of SiO<sub>2</sub> with Pt and Cr electrodes printed via lithography is used. NWs are grown between the electrodes to establish contact, allowing for the measurement of their electrical resistance. The sensor features two pads for resistance measurement, which are connected to the sensor electrodes. The electrodes form parallel tracks alternating with the pads and are separated by distances of 2.5 μm, 5 μm, and 10 μm.

The precursor and substrates are placed on a rectangular fused quartz sheet. Fig.(2) shows the distribution of the precursor and substrates along the tube in one of the experiments. The gas enters the chamber from left to right. The first element is a fused quartz boat containing 1 g of 99.99% tin powder. Further along are the samples. The square samples correspond to the Si/SiO<sub>2</sub> substrates, and the transparent rectangular samples are the chips intended for sensor fabrication. At the end, two square samples are placed on top of a rectangular ceramic boat.



**FIG. 2:** Distribution of precursor and samples along the furnace.

## B. Characterization and gas sensing

The samples were analysed using the Jeol-7100 Field Emission Scanning Electron Microscope (FE-SEM), operated at 10 keV.

To study the sensor's behaviour in the presence of gases, a gas station was used. This station is a rectangular custom-made stainless-steel chamber of 8.6 mL where the LED and the chip are placed one above the other without touching. The cavity has a gas inlet and outlet. At the inlet, there are four MFCs that regulates the flow of gases (all the experiments were conducted at a constant flow of 200 mL/min). One of the MFC outlets is connected to a synthetic air line that passes through a bottle containing distilled water. The high-pressure air causes the water to bubble, and the RH of the resulting air can be adjusted based on the airflow rate (calibrated and monitored using a SHT85 commercial sensor). The other MFC outlets supply dry synthetic air and CH<sub>4</sub>.

To measure the sensor's response, a Keithley 2602B Source Measurement Unit (SMU) was used. This unit allows for both the polarization of the LED (with a fixed current) and the measurement of the sensor's resistance (with a fixed current too). The LED used emits at a wavelength of 360 nm.

## IV. RESULTS AND DISCUSSION

### A. Scanning Electron Microscopy (SEM)

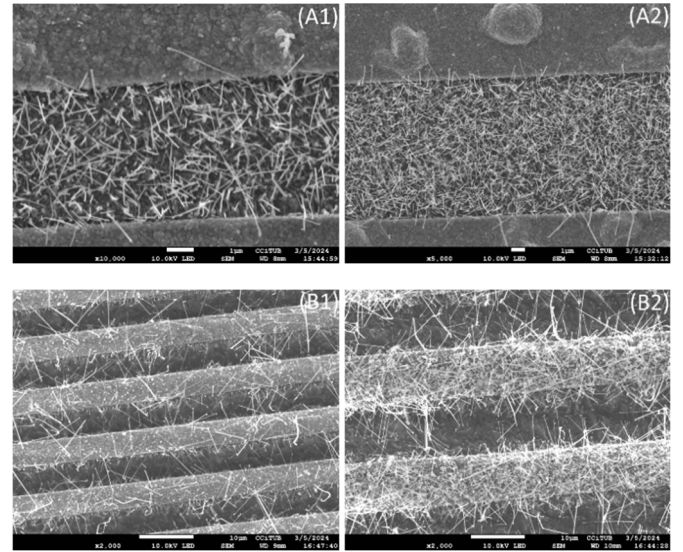
Fig.(3) (A) presents two images from an experiment conducted at 900 °C with 0.5 g of Sn as the precursor, utilizing a gas flow of 100 sccm of 1000 ppm of O<sub>2</sub> diluted in Ar during the growth phase. The first image (A1) corresponds to the growth of NWs on a chip with a 5 μm spacing between electrodes, while the second image (A2) corresponds to growth on a chip with a 10 μm spacing. The NW growth was successful in this experiment, as the NWs spanned the electrodes, making the sensor a good candidate for gas sensing measurements.

Fig.(3) (B) shows two images from a different experiment, this time conducted at 1000 °C while maintaining the same amount of precursor and gas flow. The first image (B1) corresponds to the chip with a 5 μm spacing, and the second image (B2) to the chip with a 10 μm spacing. In this experiment, the growth was not satisfactory, as the NWs grew on the tracks but not between them, resulting in poor contact and making the sensor less suitable for gas sensing.

Various experiments were carried out during the study by changing the amount of precursor (0.25 g, 0.50 g, 1.00 g). It was observed that increasing the precursor amount improved NW growth, with the best results obtained using 1.00 g. The criteria followed include the length, diameter, and growth density of the NW between the electrodes. Longer, thinner, and more densely grown NWs result in a better sensor response due to a larger variation in resistance.

Additionally, experiments were carried out by varying the O<sub>2</sub> concentration from 0 to 210 kppm (21% O<sub>2</sub> using synthetic air), but none yielded favourable results. Increasing

the O<sub>2</sub> concentration resulted in the growth of porous structures rather than NWs. Conversely, reducing the O<sub>2</sub> concentration resulted in low-quality NWs (very short and thick) with mainly horizontal growth.



**FIG. 3:** SEM images from the first experiment (A) and the second experiment (B). The first chip has a 5 μm spacing, and the second chip has a 10 μm spacing.

### B. Gas Sensing

Before studying the sensor's behaviour in the presence of gases, an initial electric characterization was performed in dry air. The LED was operated at a constant intensity while varying the current applied to the sensor from -2 mA to 2 mA. Fig.(4) shows the resulting I(V) curves. It can be observed that the sensor exhibits a dual Schottky behaviour (metal-semiconductor-metal junction) when not illuminated, and an ohmic behaviour under illumination with currents equal or above 3 mA.

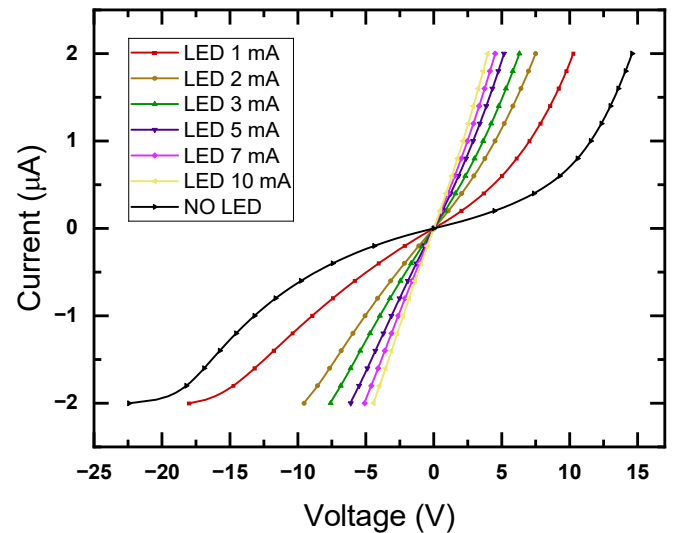


**FIG. 4:** I(V) curve of the sensor for different LED currents.

Subsequent experiments were conducted by maintaining a constant RH of the air while varying the LED intensity in increasing order: 0 mA, 1 mA, 3 mA, 5 mA, 7 mA, 10 mA, with the current through the sensor held at 1  $\mu$ A. Fig.(5) (a) shows the different curves at constant RH, where the transients can be observed when changing the LED current. The response time (Fig.(5) (b)) of the sensor was studied for each LED current transition (time taken to go from 90% to 10% of the initial value before it started to drop). It can be observed that the sensor's response time decreases as the LED intensity or humidity increases except under dry air, but the resistance variation also decreases in all cases. This behaviour might be attributed to a high photon flux causing a substantial desorption of the adhered ions, resulting in a diminished response.

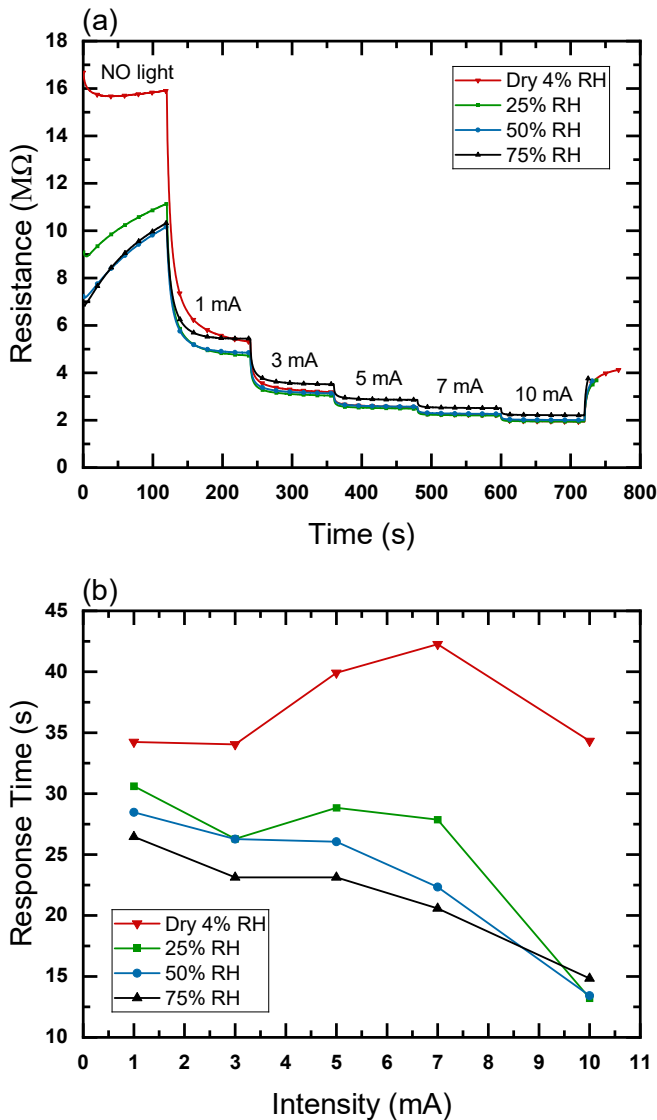


**FIG. 5:** (a) Behaviour of the sensor at different LED intensities with fixed RH. (b) Sensor response time for each LED transition.

Finally, a study was conducted using 10-minute humidity pulses to analyse the sensor's behaviour. Fig.(6) shows the sensor's response with the LED current fixed at 0 mA, 3 mA, and 7 mA, and the sensor current fixed at 1  $\mu$ A. It is worth to note the p-type behaviour of the sensor when illuminated by the LED. It can be observed that when the sensor is exposed to humidity pulses without illumination, the resistance decreases, whereas it increases under illumination for the two tested light intensities. It is possible that the UV light is dissociating water molecules, thereby increasing the number of adsorbed O<sub>2</sub><sup>-</sup> ions. In addition to using humidity pulses, CH<sub>4</sub> pulses were also tested, but the sensor did not respond to the gas.

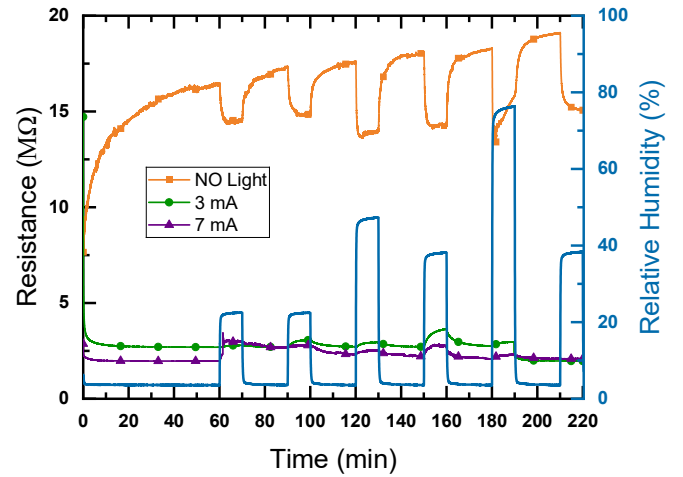


**FIG. 6:** Sensor response to humidity pulses with fixed LED intensity at a constant temperature of 25.8 °C.

## V. CONCLUSIONS

In this study, we fabricated SnO<sub>2</sub> NW-based gas sensors. The optimal fabrication conditions were 900 °C, 1 g of Sn as the precursor, and 100 sccm of 1000 ppm of O<sub>2</sub> diluted in Ar as the carrier gas. Regarding gas measurements, in dry air, the I(V) characteristics of the sensor exhibited Schottky behaviour (metal-semiconductor-metal junction) when not illuminated, and an ohmic behaviour under illumination with currents above 3 mA. Subsequently, the sensor's response was examined in the presence of humid air at different fixed RH with increasing LED intensity. It was found that both the response time and the relative change in electrical resistance decreased as the LED intensity or humidity increased. Finally, the sensor's behaviour in dry air with humidity pulses (varying RH) was investigated. It was observed that the sensor exhibited n-type behaviour when not illuminated and p-type behaviour when illuminated. In addition to humidity pulses, CH<sub>4</sub> pulses were also tested, but the sensor did not respond.

## VI. ACKNOWLEDGEMENTS

I would like to express my gratitude to my supervisor, Paolo Pellegrino, for his dedication to my work and his valuable guidance. I would also like to thank Dr. Guillem

Domènech Gil for everything he has taught me about SnO<sub>2</sub> NW fabrication and gas sensor characterization. Finally, I

would like to thank my family for financing my studies as I would not have made it here without them.

- 
- [1] Emanuel P. Nascimento, Hellen C.T. Firmino, Gelmiros A. Neves, Romualdo R. Menezes, "A review of recent developments in tin dioxide nanostructured materials for gas sensors", *Laboratory of Materials Technology (LTM), Department of Materials Engineering, Federal University of Campina Grande, Campina Grande, PB, Brazil*.
- [2] J.D. Prades, R. Jimenez-Diaz, F. Hernandez-Ramirez, S. Barth, A. Cirera, A. Romano-Rodriguez, S. Mathur, J.R. Morante, "Equivalence between thermal and room temperature UV light-modulated responses of gas sensors based on individual SnO<sub>2</sub> nanowires", *Sensors and Actuators B 140 (2009) 337-341*.
- [3] Jasmin-Clara Bürger, Sebastian Gutsch, Margit Zacharias, "Extended View on the Vapor–Liquid–Solid Mechanism for Oxide Compound Nanowires: The Role of Oxygen, Solubility, and Carbothermal Reaction", *Department of Microsystems Engineering IMTEK, Laboratory for Nanotechnology, University of Freiburg, Georges-Köhler-Allee 103, 79110 Freiburg, Germany*.
- [4] Monika Kwoka, Barbara Lyson-Sypien, Anna Kulis, Dario Zappa, and Elisabetta Comini, "Surface Properties of SnO<sub>2</sub> Nanowires Deposited on Si Substrate Covered by Au Catalyst Studied by XPS, TDS and SEM", *Nanomaterials 2018, 8, 738*.
- [5] Ming-Ru Yang, Sheng-Yuan Chu, Ren-Chuan Chang, "Synthesis and study of the SnO<sub>2</sub> nanowires growth", *Sensors and Actuators B 122 (2007) 269–273*.
- [6] Le Viet Thong, Nguyen Duc Hoa, Dang Thi Thanh Le, Do Thanh Viet, Phuong Dinh Tam, Anh-Tuan Le, Nguyen Van Hieu, "On-chip fabrication of SnO<sub>2</sub>-nanowire gas sensor: The effect of growth time on sensor performance", *Sensors and Actuators B 146 (2010) 361–367*.
- [7] Maria Vesna Nikolic, Vladimir Milovanovic, Zorka Z. Vasiljevic, Zoran Stamenkovic, "Semiconductor Gas Sensors: Materials, Technology, Design, and Application", *Sensors 2020, 20, 6694*.
- [8] Ying Wang, Li Duan, Zhen Deng and Jianhui Liao, "Electrically Transduced Gas Sensors Based on Semiconducting Metal Oxide Nanowires", *Sensors 2020, 20, 6781*.
- [9] M. Meyyappan and Mahendra K. Sunkara, "INORGANIC NANOWIRES: Applications, Properties, and Characterization", *CRC Press, Taylor & Francis Group*.